WORLD CONFERENCE ON TIMBER ENGINEERING 2025
BRISBANE, AUSTRALIA
Advancing Timber for the Future Built Environment

DESIGN OF A TIMBER DIAGRID SEISMIC STRUCTURAL SYSTEM

Jaimie Whitehead[1], Hamish Strange[2], Nicki Vance[3]

ABSTRACT: This study outlines the design approach of a 3-storey unconventionally shaped office building at Fisher & Paykel Appliances new headquarters in Auckland, New Zealand, using the recently published NZS AS 1720.1:2022 - Timber Structures Part 1: Design Methods. When completed, the diagrid building will be one of the largest mass timber office buildings in New Zealand, with a floor area of over 12000m^2. Due to the unusual geometry of the building, the application of EYM and brittle failure mechanisms were verified through two full scale tests of the node of the lateral load resisting diagrid structure. The testing demonstrated the brittle failure mechanisms in NZS AS 1720.1 were suppressed, but identified an additional brittle failure mode – splitting. This study also concluded that the screw stiffness appears lower than that calculated using both NZS AS 1720.1 and Eurocode, EN-1995-1-1:2004+A2:2014.

KEYWORDS: NZS AS 1720.1:2022, Seismic, Connections, Diagrid, Mid-rise

1 – INTRODUCTION

The ambitious new global headquarters for Fisher & Paykel Appliances is an architecturally-driven three-storey mass-timber building with complex – but repeating – curved geometry, named the "Home" building. The Laminated Veneer Lumber (LVL) and Cross-Laminated Timber (CLT) structure provides over 12,000m^2 of open-plan office, collaboration, and social spaces for nearly 1000 employees.

Figure 1: 'Home' building, credit: RTA Studio

Fisher & Paykel Appliances' new Home is located in Penrose, Auckland, New Zealand. The site is constrained by complex height plane planning rules and overland flow (storm flooding) throughout the site. The overland flow path drove the shape of the building, by using a natural ground depression to create a pond and landscaped oasis which the building wraps around. This central pond and surrounding landscaping acts as a catchment for floodwaters in a storm event.

New Zealand is a highly seismic region, and while Auckland has a lower seismicity than other areas of the country, the design building accelerations are approximately 0.4g for a one-in-500 year event. This means seismic actions still govern the low-rise lightweight, but stiff, timber structure over wind pressures of around 1kPa.

To achieve economic and robust buildings in a seismic region, New Zealand seismic engineering uses the concept of "ductility", where one element of the building acts as a "fuse", or "Potential Ductile Element"[4] (PDE), to reduce the design loads experienced by the other elements. This "fuse" is designed to stretch plastically, both absorbing earthquake energy and accommodating the displacement from the earthquake in one reliable (non-brittle) element. The other elements of the structure are then designed for a possible "overstrength" force from the PDE "fuse" considering material variation and strain hardening – this is termed "capacity design".

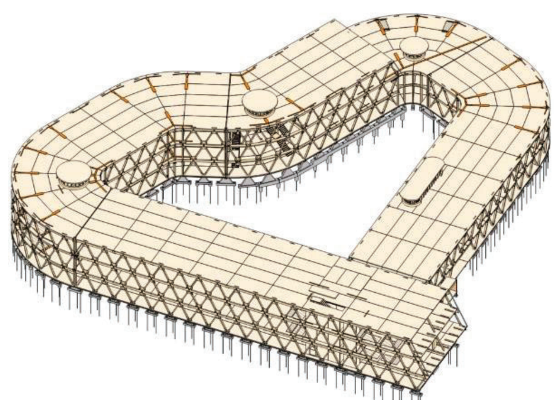

Figure 2: 3-D model of 'Home' building; perimeter diagrid

In New Zealand, it is typical for a client to directly employ the design team for the complete design process from concept stage to final detailing of connections, as well as during construction. When this end-to-end design approach is combined with the "fuse" concept, it is important to consider primary connection details early in

[1] Jaimie Whitehead, Dunning Thornton, Wellington, New Zealand, dtcwgtn@dunningthornton.co.nz

[2] Hamish Strange, Dunning Thornton, Wellington, New Zealand, dtcwgtn@dunningthornton.co.nz

[3] Nicki Vance, Dunning Thornton, Wellington, New Zealand, dtcwgtn@dunningthornton.co.nz

[4] This terminology is specific to timber design and used in NZS AS1720.1:2022.

https://doi.org/10.52202/080513-0649

the design process. This was a particularly important philosophy for the unusual mass-timber design and the scale and geometry of the Home. For complex or large-scale projects, a second structural engineer is often engaged as a peer reviewer to discuss and agree design principles and detailing. For Home, PTL Structural & Fire (timber design specialists) was the structural peer reviewer in a very collaborative and sometimes philosophical design process, with a strong focus on the diagrid connection design.

2 – STRUCTURAL FORM

The structural form consists of an LVL diagrid structure wrapping both interior and exterior perimeters of each of the four 16-metre-wide buildings. 295x180 LVL braces on a 2:1 angle run on a 4 metre module and provide both gravity support to the floors and roof as well as act as the lateral load-resisting system, refer Figure 4. Across the ribbon width, pairs of 590mm x 236mm LVL primary beams provide gravity support to 590mm x 177mm LVL secondary beams and the 210mm thick 5-layer CLT floor, detailed in Figure 5. These beams, at 8 metre centres, are supported on a 1180mm x 295mm LVL central column, creating a moment-resisting frame that forms the lateral load-resisting system across the width of the building. For context, Table 1 details New Zealand LVL properties.

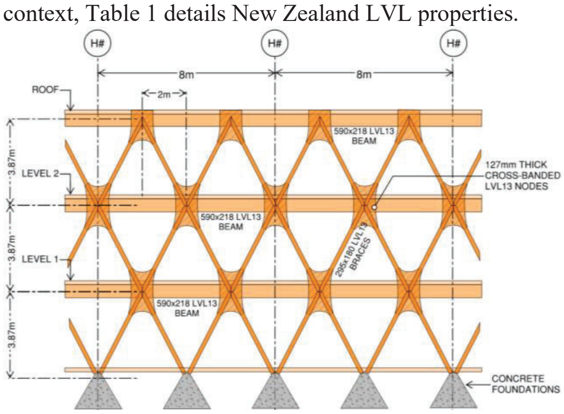

Figure 3: Elevation of typical perimeter diagrid

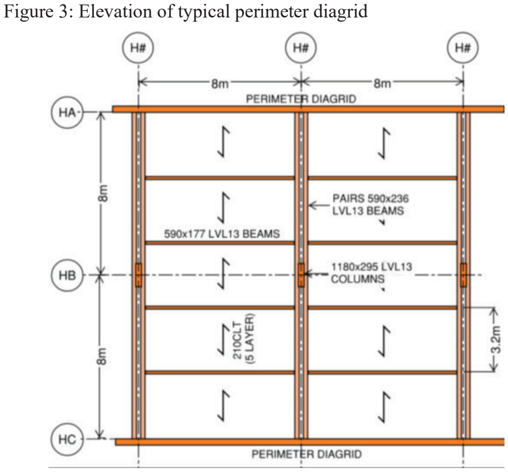

Figure 4: Typical bay floor plan (16m x 16m)

Properties	Grade	
	LVL13	*LVL13 Cross-banded*
Young's Modulus, E	13,200 MPa	13,200 MPa
Shear Modulus, G	660 MPa	660 MPa
Bending on edge, f_b	50 MPa	48 MPa
Shear on edge, f_s	4.6 MPa	4.6 MPa
Shear on flat, f_s	3.5MPa	3.5MPa
Compression parallel to grain, f_c	42 MPa	38 MPa
Compression perpendicular to grain, f_p	12 MPa	12 MPa
Tension parallel to grain, f_t	30 MPa	30 MPa
Characteristic density (for connection design)	480 kg/m^3	480 kg/m^3
Special requirements	Nil	Cross-banded lay-up

Table 1: LVL properties

The building has been structurally separated into four independent structures due to the ribbon-shaped floor plate, with movement joints to allow for thermal and seismic movement.

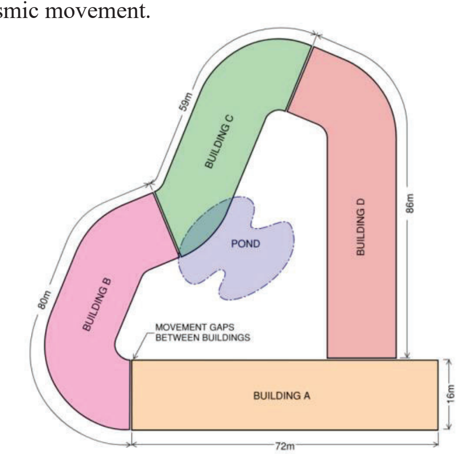

Figure 5: Plan of 'Home' - four buildings around central pond

The C- and S-shapes of the curved buildings create stiff lateral load-resisting sections of diagrid that compete with the more flexible moment-resisting frames. This load distribution creates the largest forces in the diagrid members that form the curves of the buildings highlighting the importance of the PDE concept in the structure.

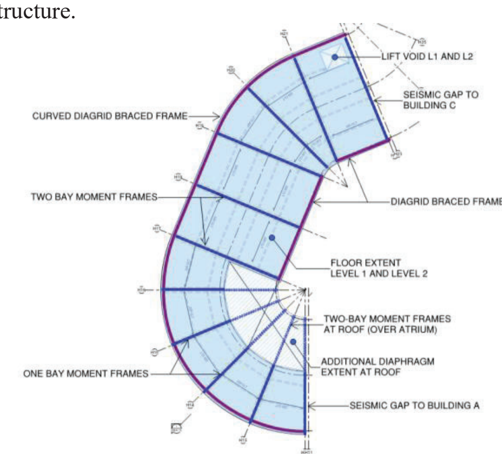

Figure 6: Lateral load resisting elements of building B

https://doi.org/10.52202/080513-0649

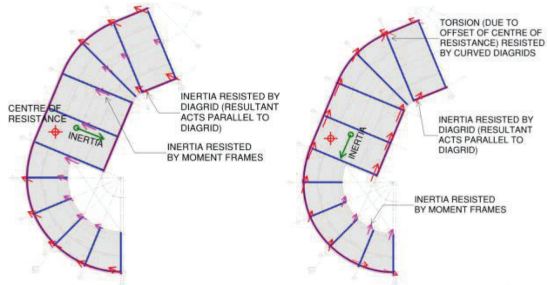

Figure 7: Lateral load resisting system for building B (L - transverse, R - longitudinal)

Connections

The project used specialist large-diameter fully-threaded engineered wood screws for the majority of the connections. This was required due to the large forces in both seismic and gravity connections, but also carried significant benefit over "off-the-shelf" non-engineered screws as material and dimensional properties are more consistent and reliable, and the screws can be placed closer together. For seismic design, the ductility of the yielding elements (screws) is also particularly important. The selection of screws was advantageous over bolts as screws could be more discreetly plugged with timber dowels which was required to meet the New Zealand building code requirements for mass timber in fire.

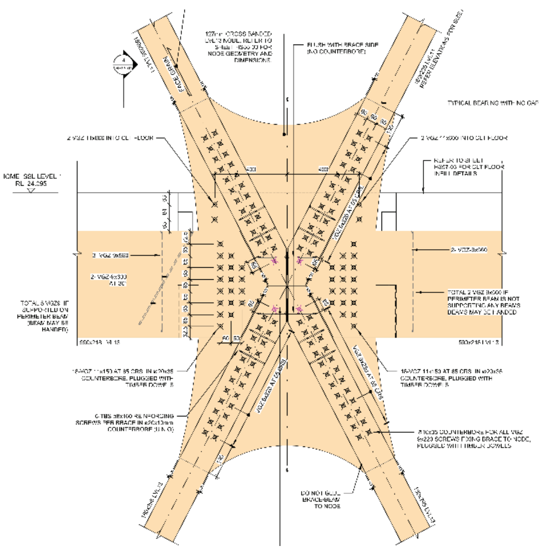

Figure 8: Construction detail of diagrid node connection

The typical diagrid connection at floor levels, shown in Figure 8, was configured with the incoming 295 x 180 LVL braces slotted over a 127mm thick central cross-banded flat LVL "node", fastened in place with two rows of Rothoblaas VGZ 9mm diameter by 220mm long fully-threaded screws, with a maximum of 24 screws per brace. Screw heads were plugged 35mm deep for the 40min fire rating requirement, so the screw was central in the brace depth. Around the curved portions of the building the detailing was essentially the same, but with sloping cuts in the faceting braces. This allowed for the nodes to be installed vertically and enabled more off-site pre-fabrication. As the node sets out the geometry of the whole structure, buildability and tolerance were essential considerations due to the diagrid's length and continuity. Critical tolerance interfaces were identified and generous tolerance provided in less critical locations. Construction in New Zealand is typically completed without tents or shrink-wrap, so moisture effects in Auckland's moderately humid environment also influenced tolerance and construction detailing.

The node connection transfers both gravity and seismic forces between the braces as shown in Figure 9. Compression loads are carried through timber bearing between the end grain of the braces and the cross-banded node. Brace tension forces are transferred into the node through the screws in double shear. There are horizontal and vertical shears generated from the tension and compression forces crossing the node. Cross-banded LVL was selected for this element to avoid perpendicular-to-grain tension, with 12 cross-banded layers.

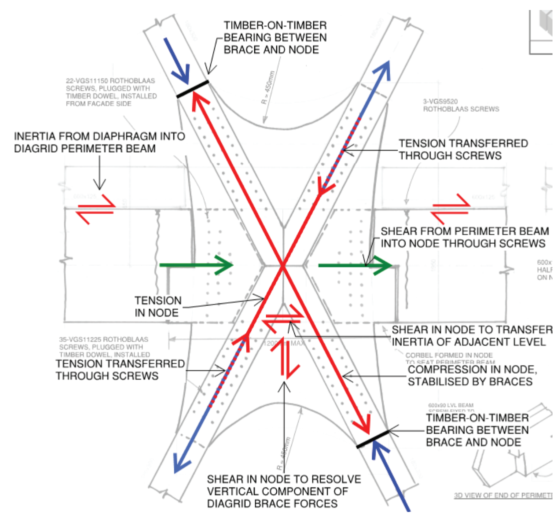

Figure 9: Seismic load paths through diagrid node

3 DESIGN METHOD FOR DIAGRID

The recently published New Zealand timber design standard (NZS AS 1720.1:2022) [1] was adopted for the timber connection design for the Home. Chapter ZZ9 details the seismic design requirements for timber buildings, introducing the terms "Potential Ductile Element" (PDE) and "Capacity Protected Elements" (CPE). The screws between the braces and the node of the diagrid were selected as the PDE. This was appropriate for the expected relatively low ductility demand expected for the structure – a maximum global ductility of 1.5. The remainder of the node connection and all other structural members are CPEs, and are designed for the potential overstrength of the screw connection, which was taken as 1.6 times the design capacity of the screw group.

https://doi.org/10.52202/080513-0649

3.1 DIAGRID NODE CONNECTION DESIGN

NZS AS 1720.1 includes "Detailed Methods" for the design of connections which are to be used for connections that are PDEs, based on the European Yield Model (EYM), and also introduces brittle failure modes for dowel-type fasteners. In a seismic context, suppression of brittle failures is needed to ensure a reliable deformation-capable mechanism occurs [2].

Typically, screwed connections have a degrading response after multiple cycles due to the crushed timber but this is more pronounced in embedment-only failure modes [2] so a screw yielding mechanism was targeted.

European Yield Model Comparison

The EYM equations in NZS AS 1720.1 chapter ZZ4 appear, in principle, the same as those in Eurocode 5 – Design of timber structures (EN1995-1-1) [3], but as a part of the design and peer review process a comparison between the two methods was completed, and some important distinctions were identified. The European Technical Approval (ETA-11/0030) for the selected screws was also referenced in conjunction with EN1995-1-1.

The EYM equations in NZS AS 1720 chapter ZZ4 are modified to calculate both a "yield" and "ultimate" capacity of the fastener, as a brittle failure may occur due to larger deformations and damage to wood fibres that occurs after the fastener yields, but before it achieves the maximum EYM capacity. This is important for the potential brittle modes outlined later in this paper.

EN1995-1-1 applies a reduction for multiple fasteners in a row. The author believes this is the most significant difference in the calculated capacities.

NZS AS 1720.1 does not reduce the screw embedment length for tolerance or screw head or tip. The embedment was taken as 45mm for both methods for comparison purposes but a reduction in screw length would be significant.

Embedding strength is calculated with the same method, but only for screws at 90 degrees to the face. The screw angle to grain is less penalised in NZS AS 1720.1 (0.67 vs 0.4), and the angle to LVL veneer laminations is not considered (noting for EN1995-1-1 this is only included in the screw manufacturer's ETA). For laterally loaded screws at angles to the grain, the author recommends designers consider additional reduction in capacity to NZS AS 1720 values.

The rope effect component of the EYM equations is entirely different. The contribution of the rope effect to the lateral capacity is significantly less when calculated using NZS AS 1720.1. [5]

In Australia and New Zealand, there are many different reported densities of radiata pine. The density of LVL was taken as 480kg/m^3 (Table ZZ8.1, NZS AS 1720.1:2022) which is the lower 5th percentile of density of New Zealand-sourced LVL at 12%MC, which is specifically used for calculation of connection capacity. Refer to [4] for clarification of the correct application of different types of timber densities in New Zealand.

Some of the NZS AS 1720.1 equations require screw properties, such as the screw tensile capacity. In New Zealand, non-engineered or "off-the-shelf" screws are commonly used. Information is not readily available for these screws, and as such these equations should only be used for screws with known data or very conservative assumptions.

The author also notes NZS AS 1720.1 refers to screws by gauge which relates to shank diameter, but the EYM equations are based on the diameter of the outer thread (consistent with the ETA). Care should be taken to use the correct diameter in the correct application.

Table 2 summarises the capacity of the fastener group calculated using AS NZS1720.1 and EN1995-1-1 considering the effective fastener factor for nails, bolts or none. The theoretical design capacity was governed by the three-hinge mechanism in all methods, with NZS AS 1720.1 producing the highest capacity.

	NZS AS 1720.1		**EN1995-1-1**		
	Yield	***Ultimate***	***Section 8.3 (nails)***	***Section 8.5 (bolts)***	***$n_{ef} = n$***
For single screw, per shear plane:					
Mode 3: One screw hinge	5040N	6080N	5670N	5670N	5670N
Mode 4: Three screw hinges	4130N	5450N	5140N	5140N	5140N
For 18 screws in double shear:					
n_{ef}	18	18	9.3	12.5	18
N_d	**149kN**	**196kN**	**96kN**	**129kN**	**185kN**
Screw slip	**0.5mm**	**2.5mm**	**1.9mm**	**1.9mm**	**1.9mm**
For 24 screws in double shear:					
n_{ef}	24	24	11.4	16.2	24
N_d	**198kN**	**261kN**	**117kN**	**166kN**	**246kN**
Screw slip	**0.5mm**	**2.5mm**	**1.9mm**	**1.9mm**	**1.9mm**

Table 2: Summary of fastener group EYM capacities

Brittle Modes

The brittle modes introduced in NZS AS 1720.1 are separated into two types; large dowel-type fasteners and small dowel-type fasteners. Small diameter fasteners deform through the timber as they reach ultimate capacity, whereas large diameter fasteners are typically governed by timber crushing and are very stiff. The threshold between small and large fasteners is a shank diameter of 6.3mm ("14g" screw[6]) (ZZ4A.1, NZS AS 1720.1). The fasteners selected have a shank diameter of 5.9mm which is near the theoretical limit of the small dowel-type fastener equations, but the outer thread diameter of 9mm

[5] The author notes a typographical error in NZS AS1720.1:2022 where the 0.25 factor has been applied in the definition of the rope effect in addition to in the EYM equation.

[6] The author notes that "off-the-shelf" screws typically have smaller diameter shanks than assumed by NZS AS1720.1.

(which is used for EYM) falls in the range for large dowel-type fasteners. As such, both failure models were assessed for this design.

The two parallel-to-grain large dowel-type fastener mechanisms considered in NZS AS 1720.1 are single row and group tear-out, shown in Figure 10 for the brace and elements. Single row tear-out is characterised by a shear failure along a shear plane on each side of each fastener row. Group tear-out is characterised by a shear failure along shear planes on the outer fasteners and a tension failure at the end of the group (as a block).

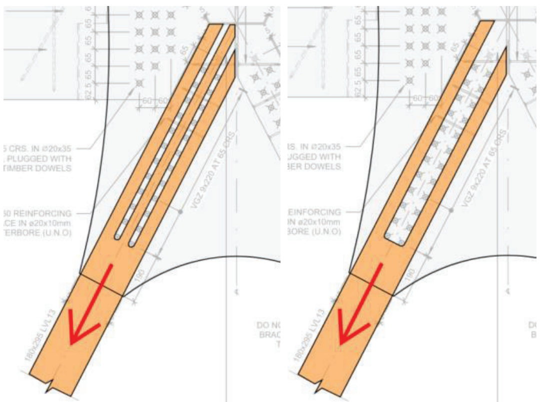

Figure 10: L - single row tear-out, R - group tear-out

The "loading surfaces factor" accounts for non-uniform shear distribution in the outer members as only one surface is loaded. The thickness of the total section is required to be engaged to fail the surface, but the embedment of the fastener was used, as the effect of partial embedment on the shear distribution is not considered in the equations.

The minimum of the end distance and fastener spacing is used to determine the capacity, so the fastener spacing was critical in achieving the capacity required. The fastener group was governed by single row tear-out due to the high tensile capacity of LVL. For further detail on large diameter dowel-type fastener failure mechanisms, refer to [5], and the equations in NZS AS 1720.1, chapter ZZ4.

NZS AS 1720.1 introduces three parallel-to-grain small dowel-type fastener brittle failure mechanisms. As small dowel mechanisms assume deformation in the fasteners, these failures are calculated by considering the relative stiffness of (and stress distribution on) three potential failure planes as shown in Figure 11; lateral shear planes (grey), bottom shear plane (green), and the head tensile area (red).

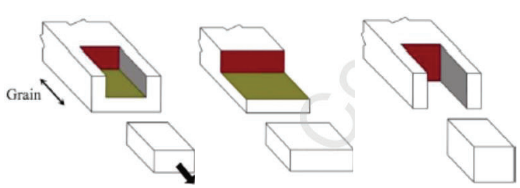

Figure 11: Small dowel-type brittle failure modes [1]

A critical variable in the small dowel-type fastener failure mechanism is the effective thickness of the section, which is calculated based on the outer thread diameter and the screw penetration. The calculated theoretical effective thickness (extrapolated) was 21mm. This was considered (and agreed with the structural peer reviewer) to be unrealistic given the likely stiffness of the squat screw, and how close the screw diameter was to the threshold for the application of the equations. The screw penetration was therefore adopted as the effective thickness (45mm).

The failure mode is interdependent on fastener spacings and end distance, and the end distance was found to be critical in achieving the capacity required, with an end distance of 190mm (21D) which is far greater than the minimum of both NZS AS 1720.1 and EN1995-1-1. The fastener group was governed by mode 1, with failure in the lateral shear area. The lateral shear area is reduced by the predrilling of fasteners, which was influential for the closely spaced screws as this gives a reduced capacity.

For detailed background on small diameter dowel-type fastener failure mechanisms, refer to [6] and the equations in NZS AS 1720.1, chapter ZZ4. These equations are based on failure modes observed in ductile rivet connections.

While other CPEs are designed for 1.6 times the design screw group capacity, it was questioned if the brittle failure modes of the PDE connection itself should be subject to the same requirement. A margin between EYM and brittle mechanisms is required to suppress them, as the mechanisms are interdependent and material variation is negated. [2] suggests 10 to 20%, and robust capacity design principles suggests some additional allowance for post-elastic stiffness. This was a strong discussion point in the structural peer review process and a margin of approximately 1.3 was agreed with prototype testing to confirm that the connection behaviour was ductile and predictable.

	NZS AS 1720.1:2022
Large dowel-type brittle failure modes	
Single row tear-out	440kN
Group tear-out	434kN
Small dowel-type brittle failure modes	
Mode 1: sides, bottom and head	324kN
Mode 2: bottom and head	598kN
Mode 3: sides and head	1058kN

Table 3: Summary of brittle failure modes

Splitting

As a result of the testing discussed later in this paper, splitting parallel to grain was also considered. Reinforcing screws across the grain were provided for 30% of the characteristic capacity of the 6 screws at the end of the fastener group as per [7] and [8]. Washer head screws were used to clamp the potential split from the axial force as well as any perpendicular-to-grain forces due to rotation of the brace due to building drift. It was agreed with the peer reviewer that reinforcement was provided for the end six screws of the brace only.

3.2 BUILDING ANALYSIS

One of the complexities of timber building behaviour – not just specific to the Home – is the significant difference in stiffness between timber-to-timber load paths (bearing

https://doi.org/10.52202/080513-0649

of the brace on the node) and connection load paths (screws in shear). Deformation from connections can have considerable impact on the effective stiffness of a member, and cannot be ignored in seismic analysis. The building stiffness impacts the fundamental period and therefore the loads experienced during a seismic event (resonance), and also the displacement.

This stiffness differential was explicitly accounted for by calculating the additional displacement screw slip of the connections at the design capacity using both NZS AS 1720.1 and EN-1995-1-1. AS NZS1720.1 provides a backbone "tangent" stiffness, whereas EN-1995-1-1 provides a secant stiffness, so these stiffnesses have been used to bound the analysis (Figure 12). The tension stiffness of the braces – calculated as a spring in series – was in the order of 20% to 50% of the compression stiffness.

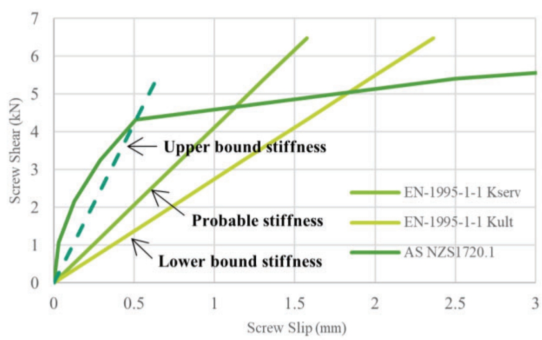

Figure 12: Screw stiffness used in analysis

Brace type	Compression stiffness kN/m	Effective tension stiffness kN/m		
	All cases	*Upper bound stiffness*	*Probable stiffness*	*Lower bound stiffness*
High *≥20 screws 200kN to 260kN*	170,000	93,000	62,000	48,000
Medium *12 > 20 screws 130kN to 200kN*	170,000	76,000	47,000	35,000
Low *≤ 12 screws <130kN*	170,000	57,000	33,000	24,000

Table 4: Effective brace stiffnesses used in analysis

Each of the four buildings were first analysed with a hand approximation, and then in three dimensions using the structural analysis programme, ETABS. A non-linear static load application was selected so that the different tension and compression stiffnesses shown in Table 4 could be analysed using a multilinear elastic link.

The distribution of forces applied in the static load case was determined using a response spectrum analysis (modal superposition), which is typically required by the New Zealand loadings design standard for irregular buildings. As response spectrum uses effective stiffness, this was taken as the average of the tension and compression stiffnesses, and the periods of the primary modes were verified with a pushover in each direction. The response spectrum analysis also demonstrated stiffness of the diagrid form had negligible higher mode effects.

4 – FULL-SCALE PROTOTYPE TEST

Two full-scale prototype tests of a node connection were conducted to verify the design, as the arrangement of the structural is unusual, with the angled braces creating unconventional geometry, and the materials are used in an innovative way. This also provided an opportunity for an invaluable buildability review with the timber contractor as there are 337 node connections in the building.

The node was set up to best emulate its 'real' performance in the application of the structure and the configuration represents a highly loaded brace configuration at level 1 in the building. A summary of the setup is shown in Figure 13. The tension braces are connected to the main cross-banded node with 18 and 24 Rothoblaas VGZ9220 fully threaded screws and the compression braces are connected with 16 and 8 VGZ9220 screws. The 24 VGZ9220 screw connection was reinforced in the second test only with 6 TBS8160 screws. The beams are connected with 18 VGS11150 screws as per the typical detail. Tension and compression forces were applied directly to the upper braces to replicate the load from the levels above. A horizontal force was also introduced via a compression and tension load each side of the node to replicate the inertia from level 1.

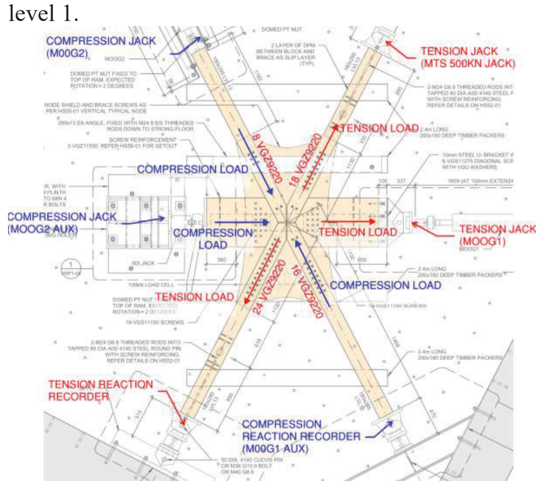

Figure 13: Prototype test set-up

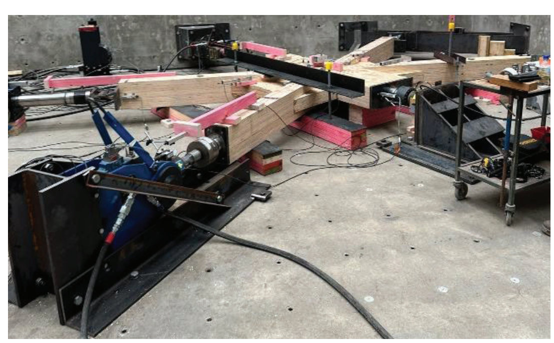
Figure 14: Prototype test set-up

Loading Protocol

Table 5 outlines the loading protocol for the test. This loading protocol outlines the applied loads in the rams, the expected reactions at the support points, and provides notes on the expected failure mechanisms as the test proceeds. The steps are reported as a percentage relating to the expected overstrength of the group of 24 screws, i.e. the design load for the capacity protected elements (CPEs) of the node.

Step	Applied Loads at Rams (kN)				Brace Reactions (kN)		Hold Time	Notes
	MTS	*M00G2*	*Flatjack*	*M00G1*	*Tension*	*Comp.*		
10%	26	17	8	8	42	33	2mins	
20%	51	34	15	15	84	67	2mins	
30%	77	51	23	23	125	100	2mins	
40%	102	68	30	30	167	134	2mins	
50%	128	86	38	38	209	167	2mins	
60%	153	103	45	45	251	201	2mins	
~65%	159	107	47	47	261	209	5mins	Nominal EYM capacity of screws
70%	179	120	53	53	293	234	5mins	
80%	204	137	60	60	335	267	5mins	Nominal brittle capacity of joint
90%	230	154	68	68	376	301	5mins	
100%	255	171	75	75	418	334	10min	Nominal capacity of node (in shear) and overstrength of screws
0%							N/A	
100%	255	171	75	75	418	334	20min	Use sequence above with 2min hold at each step.
110%	281	188	83	83	460	368	10min	
120%	306	205	90	90	502	401	10min	Increase load incrementally until node or screw failure occurs
200%	500	250	100	100	718	468	N/A	Max capacity of all rams

Table 5: Prototype test loading protocol

5 – TEST RESULTS

Test 1

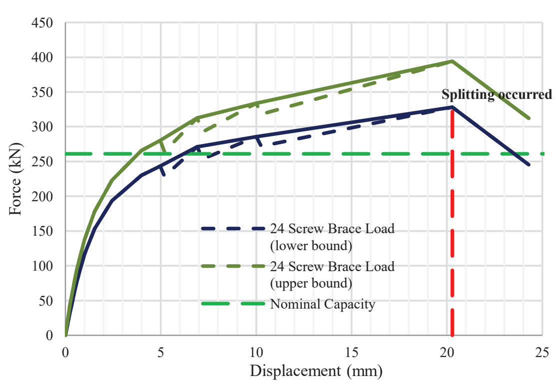

Figure 15: Test 1 - Force-displacement of 24 screw brace

Table 7 summarises the displacement and load in the 24 screw brace during test 1, and observations noted during the testing. Figure 15 shows the force-displacement plot for the 24 screw brace. Splitting along the screw line occurred at 90% of the target load (which was the calculated overstrength of the screw connection).

Step	Disp. of node (building drift)	24 screw brace		Observations
		Tension load	*Screw slip (local ductility)*	
<50%	15mm (0.4%)	208kN	2.44mm	No significant noises, no indication of screw movement at heads. Gap closed at bearing at compression brace, localised crushing.
65%	20mm (0.5%)	261kN	4.97mm (~1.0)	Rotation of screw heads.
80%	35mm (0.9%)	309kN	10.0mm (2.0)	Creaking noises. Further rotation of screw heads.
90%	51mm (1.3%)	361kN	20.3mm (4.0)	Splitting occurred on 24 screw brace along row of screws between counterbored holes
100%	57mm (1.4%)	418kN	25mm (5.0)	Splitting extended along full screw row (Figure 17, Figure 16)
100%	62mm (1.5%)	N/A	> 25mm	Partial splitting occurred on 18 screw brace. Significant displacement of 18 screw brace (Figure 17)

Table 6: Test 1 - 24-screw brace forces, displacement, test observations

Notes on test 1:-

- The load cell on the tension brace did not record so results are approximated using other load cell records. Due to the incomplete data, lower and upper bound forces were reported.
- There are likely losses due to friction between the braces and the strong floor
- The potentiometer displacement capacity was exceeded for beyond 100% loads.

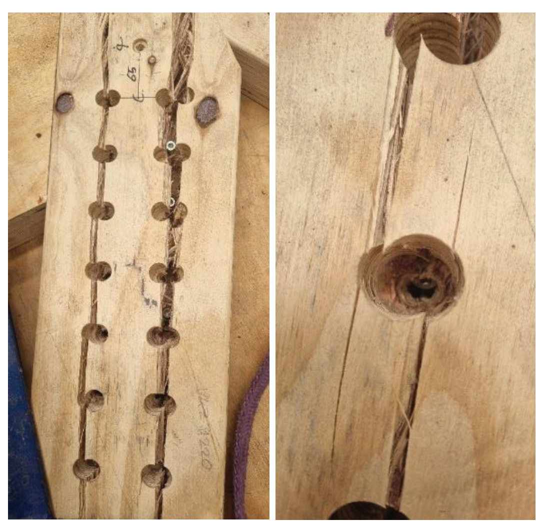

Figure 16: Close-up photos of test 1 splitting failure

https://doi.org/10.52202/080513-0649

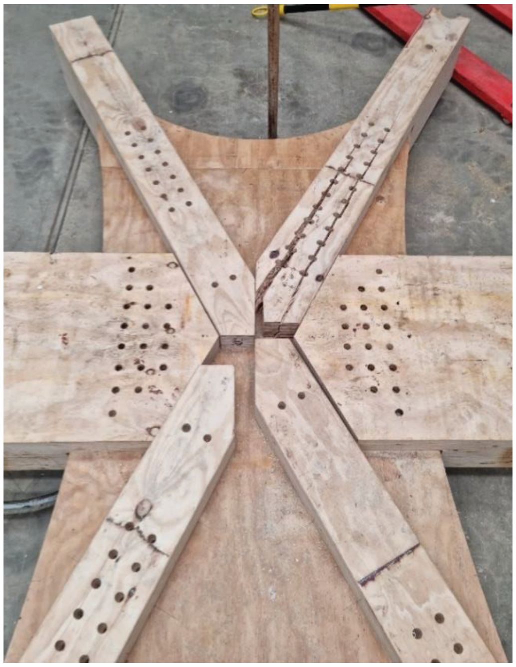

Figure 17: Photo of test 1 showing splitting of 24-screw brace (top right) and significant displacement of 18-screw brace (bottom left)

Test 2

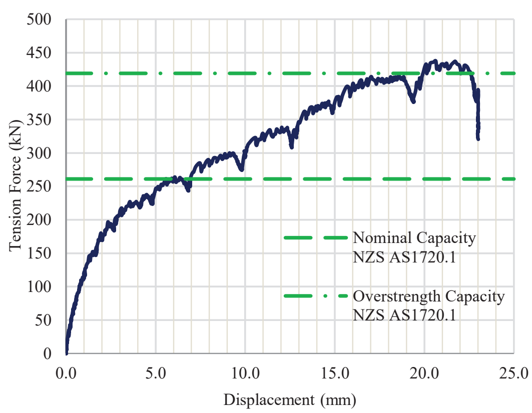

Figure 18: Test 2 - Force-displacement of 24-screw brace

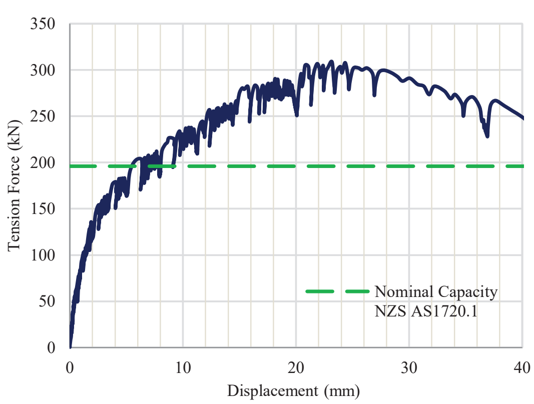

Figure 19: Test 2 - Force-displacement of 18-screw brace

Confinement (anti-splitting) screws were added (to the 24 screw brace only) for the second test to suppress the brittle splitting failure observed in test one. Table 7 summarises the displacement and load in the 24 screw brace, and observations noted during the testing. Figure 18 and Figure 19 show the force-displacement plot for the 24 screw brace and the 18 screw brace.

Step	**Disp. of node (building drift)**	**24 screw brace**		**Observations**
		Tension load	***Screw slip (local ductility)***	
<50%	15mm (0.4%)	190kN	2.5mm	No significant noises, no indication of screw movement at heads. Gap closed at bearing at compression brace, localised crushing.
65%	20mm (0.5%)	235kN	4.6mm (~1.0)	Rotation of screw heads in 24 screw brace.
80%	30mm (0.7%)	296kN	9.3mm (2.0)	Creaking noises. Rotation of screw heads in 24 screw brace.
90%	35mm (0.9%)	337kN	12.3mm (3.0)	Creaking noises continued. Further rotation of screw heads in both 24 screw and 18 screw brace.
100%	40mm (1.0%)	371kN	14.7mm (3.2)	Creaking noises continued. Further rotation of screw heads. Evidence of 18 screw brace strengths displacing significantly over this load step.
120%	55mm (1.4%)	437kN	20.6mm (4.5)	Cracking noise. Hairline split occurred in 18 screw brace between 3 screw counterbores. Localised splitting at notch in brace. Figure 20.
>120%				Continued displacement in 18 screw brace. Figure 21.

Table 7: Test 2 - 24-screw brace forces, displacements, observations

Notes on test 2:

- Friction between restraint angle and 18-screw brace increased as brace widened. Results beyond 120% likely have some false "rope effect" due to this.
- Some friction between braces and strong floor. Mitigated in test 2 using 2 layers of DPC but some evidence of ~5 to 10% discrepancy in brace force.

Figure 20: Test 2 - L: splitting between screws in 18-screw brace, R: splitting parallel to laminations at notch in brace

https://doi.org/10.52202/080513-0649

Figure 21: Test 2 - L: Screw heads at end of test, R: screw displacement through brace at end of test

6 DISCUSSION

Discrepancies in strength and stiffness

The approximate yield capacity of the screws appeared to be lower than that calculated using NZS AS 1720 in both tests, noting the significant post-yield stiffness makes it difficult to pinpoint the true "yield" point. Table 8 compares the calculated capacity and the test results which are reported raw.

In the first test, splitting occurred along the screw line at larger displacements, possibly amplified by the rotation of the brace creating perpendicular-to-grain forces, whereas no splitting occurred in the second test with the reinforcing screws. Currently splitting (when loaded parallel to the grain) is not considered by NZS AS 1720.1, and the author believes this is a critical unreliable mechanism that is simple to suppress, referring designers to [8] for more guidance on reinforcing connections. Additionally, there is no effective fastener factor in NZS AS 1720.1. The author believes that in the absence of anti-splitting reinforcement, a reduction factor for the number of fasteners in a row should be included. But, for connections that are PDEs, it is strongly recommended that the connection is reinforced, to suppress potential splitting and to avoid underestimating the overstrength of the connection for capacity design procedures.

A single hinge mechanism appeared to occur. It is the authors opinion that the embedment length assumed in NZS AS 1720.1 is too long, and some reduction in screw length should be considered for screw heads and tips similar to European procedures (ETA / Eurocode). It is noted that the screw embedment was at the limit of 5D, which likely contributed to this discrepancy. This was a design decision to provide the full encapsulation of the screw for fire as per AS NZS 1720.4.

The predicted small diameter dowel-type fastener brittle mechanism did not occur. The author believes this is likely due to the stiffness of the short, squat fastener. The large diameter dowel-type fastener mechanisms appeared to be more appropriate for the screw arrangement. The calculations and test results raised the following questions about the small diameter dowel-type fastener brittle methods presented in NZS AS 1720.1;

- Should the effective thickness, for short squat fasteners converge with the full fastener embedment as the stiffer fastener would more equally load the timber?
- Do the equations (based on large groups of rivets) capture the correct distribution of lateral shear for only two rows of fasteners?
- Are the equations suitable for engineered wood screws with large outer thread to shank ratios? The author understands that the equations are intended for "off-the-shelf" screws.

The observed post-yield increase in strength was likely due to the rope effect as the screw displaced, providing significant residual capacity in the screw connection. The rope effect contribution calculated using NZS AS 1720.1 was lower than that calculated using EN1995-1-1, and this may be an underestimation.

The testing showed the screw stiffness was much less than that calculated by both NZS AS 1720 and EN-1995-1-1, refer Figure 22. There was good initial correlation with EN1995 in the first 1mm which is logical for a force-based non-seismic design approach. There was poor correlation for the initial stiffness with NZS AS 1720 equations. In the author's opinion, these equations may be out-dated for larger diameter and engineered screw fasteners as they are based on small diameter nails. The post-yield stiffness correlated well, but demonstrates the possible over-estimation of yield capacity discussed earlier.

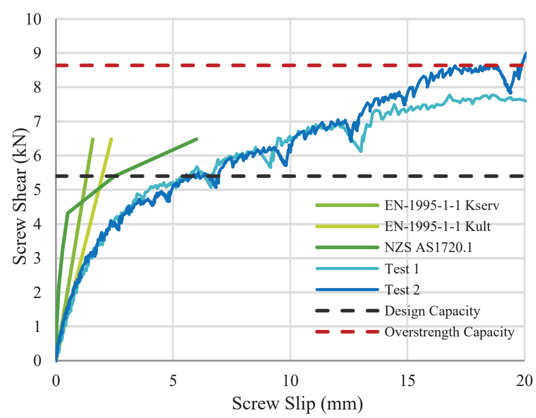

Figure 22: Test results compared with calculated stiffnesses

This may have significant impact on flexible structural forms, as a higher yield displacement means less ductility is achieved and more total displacement occurs. This could be unconservative for seismic design even when the fasteners are not used as the PDE as the elastic displacement of the system is increased through the slip of the connections. The author recommends adopting a linear stiffness (possibly EN-1995-1-1 ultimate stiffness) instead of the stiffness provided in NZS AS 1720.1.

https://doi.org/10.52202/080513-0649

	European Yield Model Capacities					**Brittle Mechanism Capacities**		**Test results**	
	NZS AS 1720.1		***Eurocode EN1995-1-1***			***NZS AS 1720.1***			
	Yield	***Ultimate***	***Section 8.3 (nails)***	***Section 8.5 (bolts)***	***$n_{ef} = n$***	***Small dowel***	***Large dowel***	***EYM***	***Splitting***
For 18 screws in double shear:									
n_{ef}	18	18	9.3	12.5	18				
N_d	149kN	196kN	96kN	129kN	185kN	324kN	434kN	180kN	270kN (test 1) 306kN (test 2)
Screw slip	0.5mm	2.5mm	1.9mm	1.9mm	1.9mm	6 to 10mm	6 to 10mm	2.5mm	14.8mm
For 24 screws in double shear:									
n_{ef}	24	24	11.4	16.2	24			N/A	N/A
N_d	198kN	261kN	117kN	166kN	246kN	324kN	434kN	250kN	328kN (test 1)
Screw slip	0.5mm	2.5mm	1.9mm	1.9mm	1.9mm	6 to 10mm	6 to 10mm	~5mm	~5mm

Table 8: Calculated capacities compared to test results

Notes:

- Values approximated off plotted results, but as plots show there is no defined “yield” or “ultimate” point so this is very subjective.

7 CONCLUSION

In the context of the Fisher & Paykel Home building;

- It was important to suppress splitting to achieve a reliable mechanism, so confinement screws were added to all braces. This was a crucial learning from the testing.
- The reduction in stiffness will be beneficial for the building due to the load distribution in the buildings with curves and the very high stiffness of the diagrid structure. Less stiffness will produce lower brace forces and therefore lower local ductility demands. As noted previously, the stiffness of the connections can be critical in the seismic design of timber structures.
- The testing showed considerable deformation capacity and local ductility. This is significantly beyond what is expected in the building, particularly given the lower stiffness of the fastener connection discussed above.

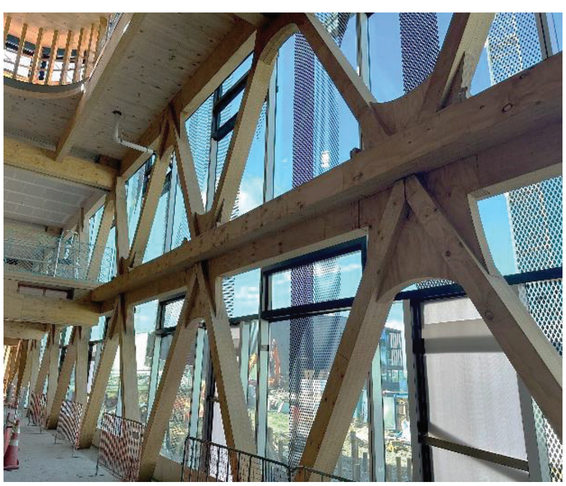

Figure 23: Construction of Home (in-progress)

The testing was an overall success, showing that the connection (with minor adjustments) will perform as intended by the design process. The valuable learnings from the testing improved the design, and provided confidence that the connection design was appropriate for the complex load distributions created by the Home’s unusual geometry.

7 – REFERENCES

[1] Standards New Zealand, Timber structures - Part 1: Design methods, Standards New Zealand, 2022.

[2] P. Quenneville and A. Hashemi, “Ductile timber connections: Understanding the factors contributing to their ductility,” in *NZSEE Annual Conference*, 2022.

[3] CEN, Eurocode 5: Design of timber structures - Part 1-1: General - Common rules and rules for buildings, 2004.

[4] Timber Unlimited, “It's all about density,” Timber Unlimited / Timber Design Society, 2024.

[5] P. Quenneville and H. Morris, “Proposal for a mechanics-based bolted connection design approach for AS 1720.1,” *Australian Journal of Structural Engineering,* vol. 9, no. 3, pp. 195-205, 2009.

[6] P. Zarnani, Load-Carrying Capacity and Failure Mode Analysis of Timber Rivet Connections, Auckland: University of Auckland, 2013.

[7] K. Kobayashi and K. Ogawa, “Measurement of Axial Force of Screws for Split Reinforcement at Timber-Steel-Timber Dowel Joint,” in *World Conference of Timber Engineering*, Oslo, 2023.

[8] Daniel Moroder and Tobias Smith, NZ Wood Design Guides Chapter 12.6 Reinforcement of Timber Members, New Zealand: NZ Wood, 2020.

https://doi.org/10.52202/080513-0649